Drosophila escape behaviours in spatially complex environments

A thesis
Submitted towards the partial fulfilment of
BS-MS dual degree programme
by

Aditya Pujari
Indian Institute of Science Education and Research
Pune

under the guidance of

Dr Gwyneth Card
Associate Professor of Neuroscience
Columbia University's Zuckerman Institute

Certificate

This is to certify that this dissertation entitled "*Drosophila* escape behaviours in spatially complex environments", submitted towards the partial fulfilment of the BS-MS degree at the Indian Institute of Science Education and Research Pune, represents original research carried out by Aditya Pujari at Columbia University, under the supervision of Dr Gwyneth Card during the academic year June 2023 to March 2024.

Supervisor: Dr Gwyneth Card
Associate Professor of Neuroscience
Columbia University

Aditya Pujari
BS-MS Student
Roll No. 20191117

Declaration

I hereby declare that the matter embodied in the report titled "*Drosophila* escape behaviours in spatially complex environments" are the results of the work carried out by me at Columbia University from the period 16-06-2023 to 31-03-2024 under the supervision of Dr Gwyneth Card and the same has not been submitted elsewhere for any other degree. Wherever others contribute, every effort is made to indicate this clearly, with due reference to the literature and acknowledgement of collaborative research and discussions.

Supervisor: Dr Gwyneth Card
Associate Professor of Neuroscience
Columbia University

Aditya Pujari
BS-MS Student
Roll No. 20191117

Acknowledgements

First and foremost, I thank my supervisor, Dr. Gwyneth Card, for her constant support, invaluable advice, and helpful discussions. Her unwavering excitement about my work has encouraged and inspired me throughout the dissertation. I would also like to thank Milo Hughes, our lab engineer, for his technical help with building the rig, as well as Dr. Han Cheong, Ehretz Gheskin, and all the Card Lab members at the Zuckerman Institute. Their kind help and support have made my life at ZI a wonderful and enriching experience, both personally and academically. And of course, I must especially thank the entire FlyCore team and GEOFF, who kept a steady supply of flies coming and without whom none of my experiments would have been possible. I am also grateful to Dr. Raghav Rajan from IISER Pune for his mentorship and support.

I would like to express my gratitude to my close friends who always believed in me even when I did not. Without their tremendous support and encouragement over the past year, it would be impossible for me to complete this study.

Finally, I would like to thank Columbia University and Kishore Vaigyanik Protsahan Yojna (KVPY) Fellowship for funding this incredible opportunity and the Indian Institute of Science Education and Research (IISER) Pune for the studentship that allowed me to conduct this thesis.

Contributions

Contributor name	Contributor role
Gwyneth Card	Conceptualization Ideas
Gwyneth Card, Aditya Pujari	Methodology
Aditya Pujari	Software
Aditya Pujari	Validation
Aditya Pujari	Formal analysis
Aditya Pujari	Investigation
Gwyneth Card	Resources
Aditya Pujari	Data Curation
Aditya Pujari	Writing - original draft preparation
Aditya Pujari	Writing - review and editing
Aditya Pujari	Visualization
Gwyneth Card	Supervision
Gwyneth Card	Project administration
Gwyneth Card	Funding acquisition

This contributor syntax is based on the Journal of Cell Science CRediT Taxonomy[1]

[1]https://journals.biologists.com/jcs/pages/author-contributions

Abstract

Escape behaviours are severely time-constrained due to fast predatory strikes. They thus provide a useful model to understand how different behaviour strategies are computed over a limited number of synapses. Broadly, one can propose two general strategies of escape: to escape away from the threat or to escape toward *safety*. While not mutually exclusive, these two strategies are fundamentally distinct in the computations they require. Escaping toward a safe place has better long-term value but might take up valuable time since it requires complex computations such as evaluating shelter locations and available escape routes. Mice escape directly towards a learned shelter location by encoding a shelter-directed vector in their brain. The proposed model behind this shelter-direction vector is closely related to models of heading direction proposed for various circuits in other animal species, including fruit flies. This thesis investigates whether fruit flies show shelter-directed escape behaviours. I tested multiple shelter designs and found that flies bias their escape trajectory towards shelters, but this bias is weak and, in the short term, does not lead to *optimal* safety-directed trajectories

Contents

List of Figures

List of Tables

1 Introduction

Defensive behaviours against predators are ubiquitous in some form or another, either as freezing behaviours aiming to avoid detection (Eilam (2005); Speedie and Gerlai (2008); Gibson *et al.* (2015); Zacarias *et al.* (2018)) or as active flight responses away from threatening stimuli (Heitler and Burrows (1977); Eilam (2005); von Reyn *et al.* (2014); Eaton *et al.* (2001). Such defensive behaviours are naturally very important for survival and are typically time-constrained due to fast predatory strikes. They are also dynamic, taking into consideration features from the environment, properties of the threat, as well as the internal state of the animal and past experiences (Blanchard and Blanchard (1971); McNaughton and Corr (2004); Dill (1974); Tammero and Dickinson (2002); Evans *et al.* (1993); Temizer *et al.* (2015); Rodgers *et al.* (1963); Vale *et al.* (2017)). Hence, contrary to naive intuition, escapes aren't always simple reactions to stimuli. They can be a powerful paradigm for studying the neural basis of complex value-based decisions and goal-directed actions, and a better understanding of how escape-relevant computations are carried out over a limited number of synapses is needed.

Broadly, one can propose two general strategies of escape: to move away from the threat or to move toward "safety" (Vale *et al.* (2017)). While not mutually exclusive, these two strategies are fundamentally distinct in the computations they require. Moving away from a threat can be implemented as a simple transformation, as observed during loom-evoked zebrafish C-start behaviour (Eaton *et al.* (2001)) or *Drosophila* takeoff responses (Card and Dickinson (2008); von Reyn *et al.* (2014)). In *Drosophila*, this response is an elaborately orchestrated behaviour comprised of at least four manoeuvres that occur sequentially while the object is approaching: freeze, a body lean or leg postural adjustment, wing-elevation, and finally, the jump (Card and Dickinson (2008); von Reyn *et al.* (2014)). When presented with dark looming stimuli on white backgrounds, the takeoff direction, determined by postural adjustment, is predominantly opposite to the direction of the looming stimulus (Card and Dickinson (2008), Fig. 1). The neural circuits converting looming stimulus locations to takeoff directions are also well understood, known to be composed of antiparallel gradients of synapses between looming-sensitive neurons and premotor neurons (Dombrovski *et al.* (2023)).

This strategy, however, has the drawback that it might not be the most adaptive solution if the animal's future position is strategically poor or if predators are able to exploit its predictable stereotypy (Eilam (2005); Catania (2010)). A good example of the latter is the predatory behaviour of

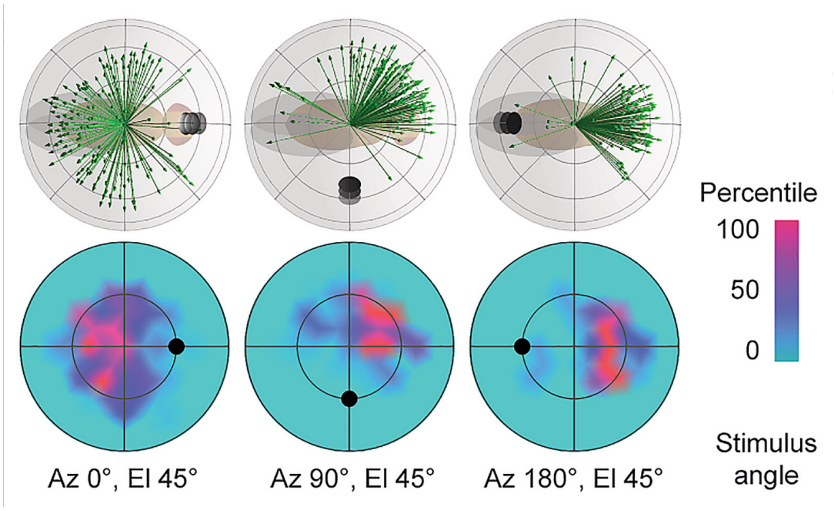

Top - takeoff direction (green arrows) in response to looming visual stimuli (dark disks) approaching from various azimuth angles. Bottom - distribution of takeoff directions with changing stimulus angles. Taken from Figure 4 from (Williamson *et al.*, 2018)

Figure 1: **Flies adjust their escape azimuth to take off away from the stimulus**

tentacled snakes, which have evolved to exploit the stereotyped C-start escape reflexes of prey. These animals place themselves in a J-shaped position and wait for prey to approach. Once a potential prey animal is close, the snake twitches muscles in the neck so the prey is startled and carries out the escape reflex directly into the snake's approaching mouth (Catania (2009, 2010)).

A better strategy is to escape towards known safe spaces in the immediate environment. Escaping towards a known safe space or shelter is costly in time since the choice of trajectory requires knowledge of the immediate environment (which is dynamic), comparing the perceived safety value of all shelters if multiple are detected, and then computing the optimal trajectory towards the shelter. Vale *et al.* (2017) showed that the primary goal of escape in mice is to reach a previously memorized shelter location. The memory of the target is generated very rapidly (within a single visit lasting 20s or less) and can be updated in response to environmental changes equally quickly. Mice have been shown to carry out this computation by maintaining a shelter-directed vector in their superior colliculus (SC) relative to the animal's head direction, allowing quick orienting responses towards the shelter followed by almost-straight flight trajectories (Campagner *et al.* (2023), 2).

Fruit flies (*Drosophila melanogaster*) are known to produce a diversity of escape behaviours (Card (2012); von Reyn *et al.* (2014); Gibson *et al.* (2015); Zacarias *et al.* (2018)). As reported earlier, they exhibit takeoffs opposite to the direction of a dark expanding circle on a white background, i.e. a looming stimulus (Card and Dickinson (2008)). However, in the presence of a wedge, takeoff directions are observed to be bimodal (2, data obtained through private communication). This suggests a shelter-directed escape phenotype since dark objects (Maimon *et al.* (2008)), as well as dark corners (Soibam *et al.* (2012a); De La Flor *et al.* (2017)) are naturally attractive to *Drosophila* and can be hypothesized to represent shelters with a high safety value in flies' natural environments.

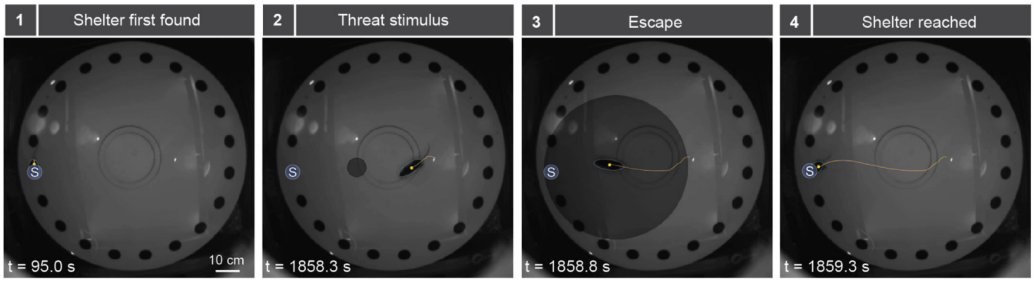

A. Mice memorize shelter locations learnt during exploration (1), and carry out shelter-directed escapes (2-4) even when the threat is located between the mouse and the shelter. Figure 1 from (Vale *et al.*, 2017)

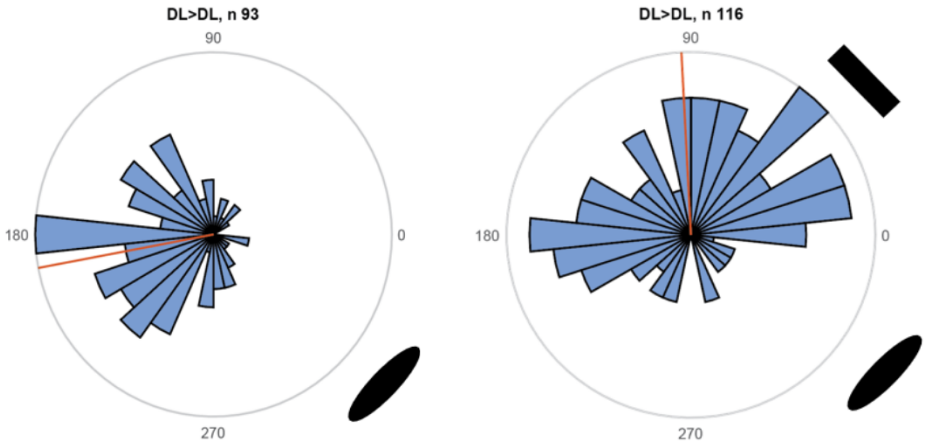

B. Flies mainly jump away from a looming stimulus (left), but show a bimodal distribution in takeoff directions showing bias towards a dark wedge (top right in second polar plot)

Figure 2: **Goal-directed escape in mice and *Drosophila***

This thesis aims to discover if flies exhibit a shelter-directed escape phenotype in open and naturalistic environments.

2 Methods

2.1 Animal husbandry and fly strains

DL *Drosophila melanogaster* (wild-type strain donated from M.H. Dickinson, Caltech) were reared on standard molasses fly food at 21.8°C temperature and 55% relative humidity on a 16hr light/8hr dark cycle. Vials containing parents were flipped every day to prevent overcrowding, and progeny were transferred to fresh vials every day to control the age of flies used in the experiments. Only 3 to 5 day old male and female progeny were used for experiments.

2.2 Behavioural apparatus (PezBowl)

All experiments were conducted in a setup henceforth referred to as PezBowl. It is built on top of the FlyPez apparatus from Williamson *et al.* (2018), adopting its stimulus presentation system. Each arena tested, barring the control, consists of an open arena for exploration and a structure meant to approximate natural shelters. The arena has a diameter and height of 30 mm and 6.35 mm, respectively. The arena for the overhang and post was 3D-printed, while the alcove was machined out from acrylic sheets 3 mm thick with two sheets placed on top of each other to obtain similar heights across all shelters.

To allow flies in the arena to perceive the stimulus and record their behaviour, this apparatus's floor and ceiling were made of transparent acrylic (3 mm thickness). The walls of the setup were coated in PTFE Plus insect-repellent coating (byFormica, Kentucky, USA) to keep the flies from walking on them. The rig was illuminated using four L300 bar lights (SmartVision, Michigan, USA), producing 850 nm wavelength IR light to evenly illuminate the arena and create high contrast between the flies and the background for good tracking. The IR lights were not visible to the fly and so in the lit arena flies could still perceive stimuli and stimuli-associated changes in brightness.

Apparatus	Description	Shelter Region
Post/Pillar	4.7 x 4.7 x 6.35 mm solid black 3D-printed cuboid	"Shadow" behind the post relative to stimulus direction
Overhang	3.5 x 3.5 mm overhang covered in black paper tape	Region directly below the overhang
Alcove	6 x 6 mm alcove outside the arena, darkened by attaching black paper tape on the outside	Region inside the alcove

Table 1: Descriptive list of potential shelters tested.

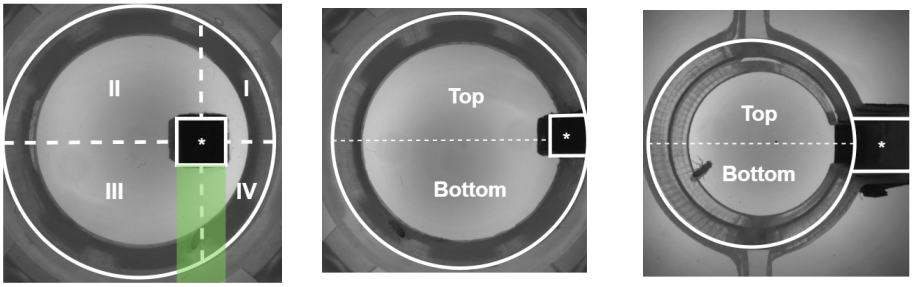

Shelter A "Post" Shelter B "Overhang" Shelter C "Alcove"

Figure 3: **Shelter designs tested** A. Numbers represent quadrants and the green shaded region represents the shadow, B and C the top and bottom halves are labelled, and the alcove and overhang are indicated by white boxes.

2.3 Experimental Protocol

The experimental protocol is described in the flowchart (4). Yellow denotes manual steps while grey denotes automated steps carried out by custom-written Python scripts.

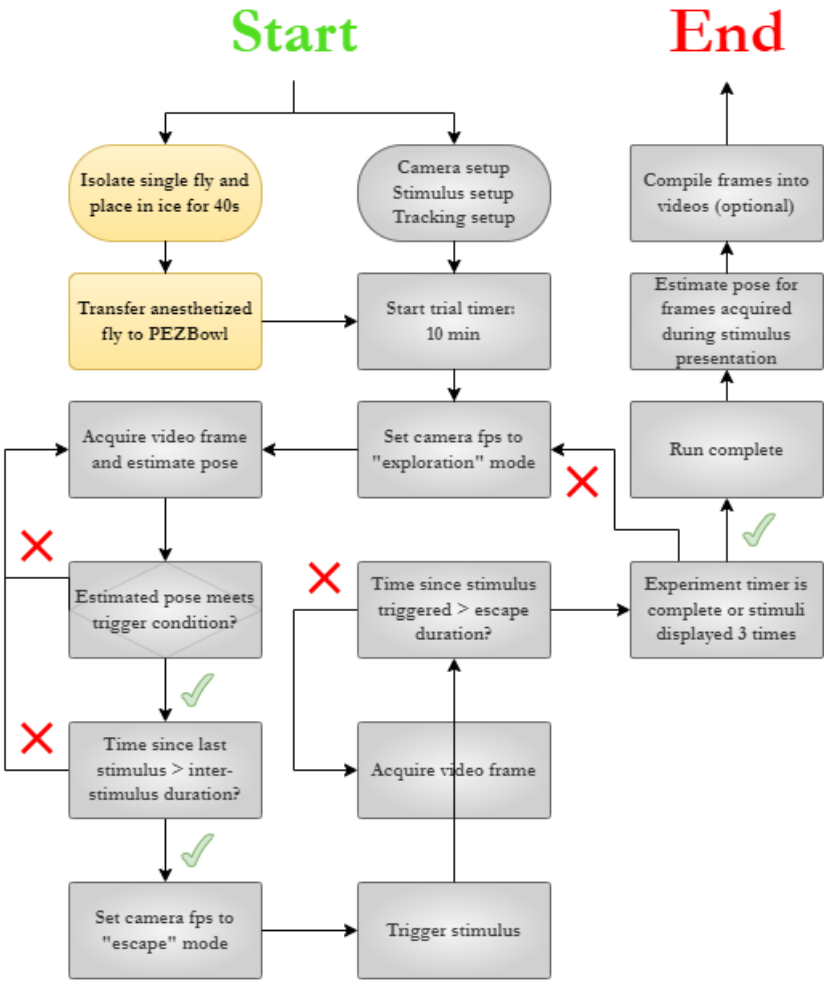

Figure 4: **Experimental Protocol**

2.4 Visual Stimulation

Looming stimuli were provided using the GlobeDisplay system developed by Williamson *et al.* (2018). The system for presenting stimuli contains a computer and projector setup which projects stimuli onto a spherical plastic screen which is surrounded by a conical mirror. The calibration of the stimulus projection onto the globe was determined empirically by measuring lines and making sure they were 10 mm apart with measuring tape prior to the start of experiments. We modified a DMD projector (DepthQ WXGA 360, Cambridge Research Systems, Rochester, Kent, UK) with an LED input (SugarCUBE model M03-005, Nathaniel Group) to display stimuli at 360hz. The looming stimuli were created to approximate a dark entity approaching

at a fixed velocity (v) with the angular size of the entity on the globe (θ) as a function of time (t):

$$\theta(t) = \tan^{-1}\left(\frac{r}{v(t)}\right) \tag{1}$$

The rate of expansion of the disk is defined by r/v, which is the ratio of the approaching entity's radius (r) to its velocity (v)(Gabbiani *et al.* (1999); Fotowat and Gabbiani (2011)). All experiments were conducted using a looming stimulus which expanded from 5° to 180° with $r/v = 40$ ms. In order to calculate size of the loom as a function of time t during analysis of escape videos, (1) was reorganised to obtain:

$$\theta(t) = \begin{cases} 0, & \text{if } t < t_{min} \\ 2\tan^{-1}\left(\frac{r/v}{t_{max}-t}\right), & \text{if } t_{min} \leq t \leq t_{max} \\ 180, & \text{if } t > t_{max} \end{cases} \tag{2}$$

where t_{min} and t_{max} are the time when the stimulus appeared on the display and the time when the stimulus reached maximum size, respectively. The stimulus was empirically measured to appear on the display 8.4 frames or $t_{min} = 56$ ms (framerate of 150) after triggering high-framerate video capture. Using this measurement and 2, t_{max} was calculated to be 972 ms. After reaching maximum size, the stimulus is displayed for a further 2 seconds, after which it disappears and is replaced by a white background. The angular size of the loom subtended at the dome's centre is given in Figure 5. The location of the stimulus on the dome is defined by two angles - the azimuth and the elevation. All stimuli were displayed at an elevation of 30°, and the azimuth varied from experiment to experiment but stayed constant per trial (i.e. per fly). A maximum of three stimuli are provided per fly, since the effects of habituation are more pronounced after four or more stimuli (Williamson *et al.* (2018)).

2.5 Video acquisition and tracking

Video data of fly responses was acquired using a PointGrey (now FLIR) FL3-U3-13Y3M-C USB-3 (Teledyne FLIR, Wilsonville, OR, USA) monochromatic camera with a -mm lens (, USA).

11 bodyparts were tracked in real-time using DeeplabCut-Live(Mathis *et al.* (2018); Kane *et al.* (2020), 6). Video capture during the "exploration" phase or between two stimuli presentations was limited to 10 frames per

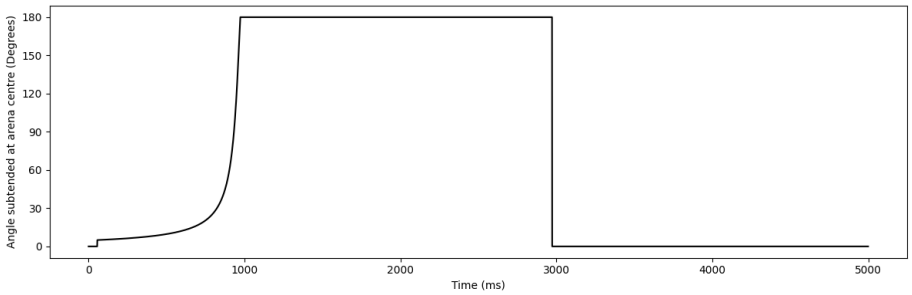

Angle subtended at the centre of the arena by the expanding disk over time

Figure 5: **Stimulus dynamics**

second because of the latency of real-time image processing and tracking by DeepLabCut-Live. Since *Drosophila* escape behaviours are carried out at very high speeds ((von Reyn *et al.*, 2014; Card and Dickinson, 2008)), after stimulus presentation live-tracking was temporarily paused to allow video capture at a higher framerate. The pose-estimation for the frames captured during stimulus presentation is done by the same DeepLabCut model after the trial is over. Trials, where no stimuli were presented either due to software failure or the fly not entering the appropriate ROI, were discarded.

2.6 Data analysis

For all designs, the shelter is comprised of a rectangular region whose coordinates are measured manually from the captured videos. The distance of the fly from the shelter/shadow was calculated as the minimum length of the orthogonal projection of the point position on the line segments defining the edges of the shadow.

All analysis and statistical tests were carried out in custom-written Python scripts. For each bodypart location estimation, DeepLabCut returns a likelihood value similar to a confidence score of the prediction by the model. All predictions with a likelihood below 0.9 were replaced with NaNs. Similarly, when a difference of more than 100 pixels was observed between adjacent predictions, both values were replaced by NaNs to preserve continuity. To create a complete trajectory from this segmented and cleaned raw data, all NaNs were replaced by imputed values using `scikit-learn` (version 1.2.0, (Pedregosa *et al.*, 2011)) ***IterativeImputer*** feature. As described in the documentation, the ***IterativeImputer*** class models each feature with missing values as a function of other features using Bayesian ridge regression, and uses that estimate for imputation in an iterated round-robin fashion for

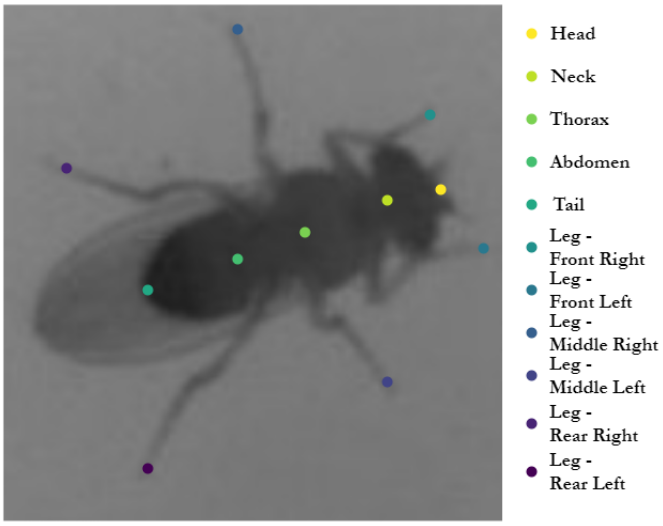

Figure 6: **Body parts labelled in real time using DeepLabCut**

the specified number of rounds. The function was run for 100 iterations as a compromise between the accuracy of imputation and time/computing costs.

The final trajectory of the flies was obtained by calculating the centre of mass of the animal at every time step, defined as the mean of the head and tail position. Every variable (path orientation, speed, distances) was calculated using this centre of mass position. The velocity along the x and y axes V_x, V_y at time t was calculated as a convolution of the change in positions at times $t-2, t-1, t$ & $t+1$ and a Gaussian kernel of size 3:

$$\begin{aligned} V_x(t) &= \begin{bmatrix} x_{t-1} - x_{t-2} & x_t - x_{t-1} & x_{t+1} - x_t \end{bmatrix} \times \begin{bmatrix} 0.25 \\ 0.5 \\ 0.25 \end{bmatrix} \\ V_y(t) &= \begin{bmatrix} y_{t-1} - y_{t-2} & y_t - y_{t-1} & y_{t+1} - y_t \end{bmatrix} \times \begin{bmatrix} 0.25 \\ 0.5 \\ 0.25 \end{bmatrix} \end{aligned} \tag{3}$$

Velocity computed in this manner results in smoother values compared to the values obtained from a discrete difference of positions. Acceleration was calculated as the discrete difference of the velocity of the fly. At every time point, three orientations θ_p, θ_o & θ_h were calculated as defined in figure 7. The orientations $\theta_p, \theta_o, \theta_h \in (-\pi, \pi)$ are calculated as defined for a standard cartesian coordinate system with the origin at the centre of the arena and stimulus always presented from a 90° direction. For escape path orientations θ_p, the angles were binned into an angular histogram distribution with 20° bins and then checked for uniformity using Rayleigh's test (also called Rayleigh's z test) of uniformity for circular data. For distributions found to be significantly non-uniform, they were fit with von Mises functions (which are close approximations to normal distributions on a circle) defined for $-\pi \leq \theta \leq \pi$ as:

$$f(\theta|\mu, \kappa) = \frac{e^{\kappa cos(\theta-\mu)}}{2\pi I_0(\kappa)} \tag{4}$$

where I_0 is the modified Bessel function of order 0. The parameters μ and κ are analogous to the normal distribution's mean μ and variance σ^2. μ is a measure of the location of the peak of the distribution, and κ is a measure of concentration around this peak. Low κ values mean a short peak and a close-to-uniform distribution, while at high values, the distribution is strongly concentrated around μ. The goodness-of-fit of the function to the distribution was assessed using Kuiper's test, which is the equivalent of the Kolmogrov-Smirnov test but crucially is invariant under cyclic transformations. In case a single von Mises function did not provide a good fit or the data clearly appeared to be multimodal, a mixture of von Mises functions was fit to the data defined (for two functions) as:

$$f(\theta|\mu_1, \kappa_1, \mu_2, \kappa_2) = \frac{e^{\kappa_1 cos(\theta-\mu_1)}}{2\pi I_0(\kappa_1)} + \frac{e^{\kappa_2 cos(\theta-\mu_2)}}{2\pi I_0(\kappa_2)} \tag{5}$$

The parameters μ and κ for all fits were computed using an Expectation-Maximization algorithm developed by François Konschelle ((Konschelle, 2021)). In case a distribution did not yield a good fit with mixtures containing up to three functions, the "best fit" amongst the mixture models tested was picked. This analysis was carried out to quantitatively describe the angular distributions, but since the peak of the von Mises functions did not always align with the peak of the histogram the exact values of μ are relatively less important than κ in describing the distributions. This analysis was only carried out for the period in time denoting "maximum activity" since we were only interested in the immediate behaviour post-stimulus and not the long-term escape paths of the flies. This period of maximum activity was calculated by

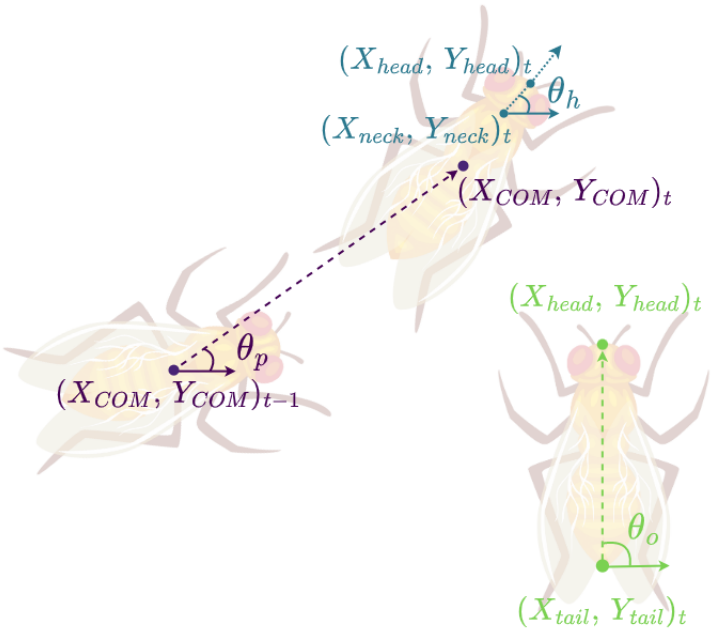

θ_p is defined as the angle between the vector defined by the centre of masses (COM) at time $t, t-1$ and the x-axis, θ_o is the angle between the head-tail vector and the x-axis, θ_h is the angle between the head-neck vector and the x-axis.

Figure 7: **Path orientation θ_p, fly orientation θ_o and heading θ_h**

obtaining time points where the mean absolute acceleration value exceeded the 90th percentile value over the entire time period. The first and last such time points, corresponding to the rapid increase and smaller decrease in velocity, were considered as t_0 and t_{end} respectively.

All parameters were tested for normality using the appropriate statistical test (Shapiro-Wilk Test and Rayleigh's Test for non-circulur and circulur data respectively). Based on the results of these tests, the choice of parametric (ANOVA) or non-parametric (Kruskal-Wallis) test was made. The results of these tests are elaborated in the Appendix (5).

3 Results

All responses to the looming stimulus were manually classified into five (exhaustive) categories. The experimenter qualitatively determined these categories, and his best judgement was used to classify escape responses:

Behaviour	**Description**
No Reaction	No behavioural reaction observed, velocity is unchanged after stimulus and any ongoing grooming behaviour is uninterrupted
Freezing	The fly abruptly ceases all motion, including grooming
Freezing & leaning	Similar to freezing, but the fly visibly leans and shifts its centre-of-mass
Sprint	Clear increase in speed in response to stimulus
Takeoff/Jump	The fly follows the stereotypical jump sequence (von Reyn *et al.* (2014)) and lands some distance away, observed as a rapid change in position within 1-2 frames

Table 2: Descriptive list of behavioural responses to stimuli

What follows is an analysis of fleeing/sprinting responses to looming stimuli in the presence of three different potential shelters.

3.1 Behaviour in environments with potential shelter - Type A ("post")

This shelter design was motivated by locust experiments ((Hassenstein and Hustert, 1999)) wherein locusts placed on a narrow pole adjusted their position so as to be covered by the pole from an approaching threat. Extending

this reasoning, this shelter consists of a large post-like object towards the side of the arena. The predicted shelter is the region directly behind the shelter relative to the stimulus (3), which can also be thought of as the "shadow" during stimulus presentations (although it is important to note that no physical shadow is present). We first checked if the presence of this potential shelter affected the choice of escape behaviour (8). The control setup is an arena without the post; post locations from the experimental group were used for analysis. Predictions about a shelter-directed phenotype include a higher number of freezing or no-reaction behaviours when the flies are closer to the shelter, as well as flies taking off or fleeing only when they are not near the shelter. The observed behavioural choices did not support these predictions. No significant difference was observed between the experimental and control groups in the distances to the shelter and the choice of behavioural response. Moreover, there was no significant difference between the median distances of flies that fled and flies that froze in response to the stimulus. A lower median distance when flies made postural adjustments and a higher median distance when flies took off only weakly supported a shelter-directed phenotype. Analysis of the speeds prior to stimulus presentation corroborates earlier work ((Zacarias *et al.*, 2018)) postulating that choice of escape behaviour is modulated by speed and flies are more likely to flee if their speed is high. The higher median and variance for sprint/fleeing behaviours and take offs is an expected result from this work. However interestingly we observed a higher median initial speed for flies that chose to freeze compared to the control (Kruskal-Wallis H test, $p < 0.01$), possibly indicating an effect of visual processing and the post on commands eliciting defensive responses. We then analysed the distribution of path orientations (θ_p, 9) during the period of rapid increase in acceleration and velocity. The purpose of narrowing down the time period was to look at instinctive responses to stimuli instead of long-term trajectories that might end up at the shelter purely due to the constraints of the arena. Since the relative location of the shelter varies based on the location of the fly, we split the trajectories based on the quadrant of the arena where the fly initiated the escape (3). In the presence of the post, escape path orientations of flies in the bottom half of the arena (quadrants III and IV) were biased towards the shelter. Interestingly this difference was multimodal for flies in quadrant III, where the peaks were either directly away from the stimulus, biased towards the shadow or directly opposite to the shadow. For quadrant IV the trajectories were more strongly biased towards the shadow. A similar but weaker directional bias in the control group is more likely the result of the curved boundary wall biasing the trajectory into the shadow. For flies in quadrants I and II, the flies mainly escaped forward and/or away from the stimulus in the presence of the post, while

in the control, they clearly escaped opposite to the stimulus. We checked if this bias was preceded by microscale adjustments in heading and orientation (θ_h & θ_o) relative to the shelter before initiating escape (Figure 10). We observed a uniform distribution of relative heading and orientation changes, which implies that the flies did not particularly orient themselves or their heads towards the shadow before initiating escape (Figure 10, Rayleigh's test, $p > 0.05$).

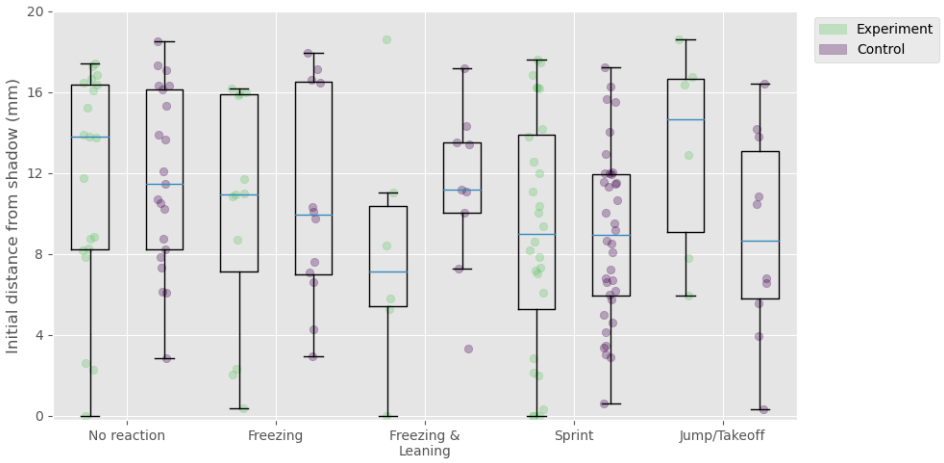

Distance from shelter immediately prior to stimulus presentation for each behavioural reaction

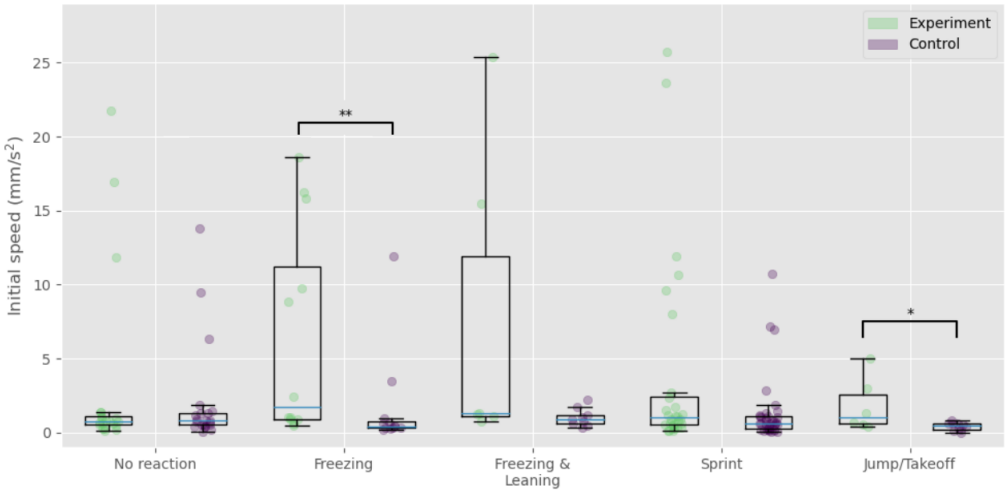

Speed immediately prior to stimulus presentation for each behavioural reaction (Kruskal-Wallis H test, * $p < 0.05$ ** $p < 0.01$)

Figure 8: **Flies don't significantly alter choice of behaviour in the presence of the post.**

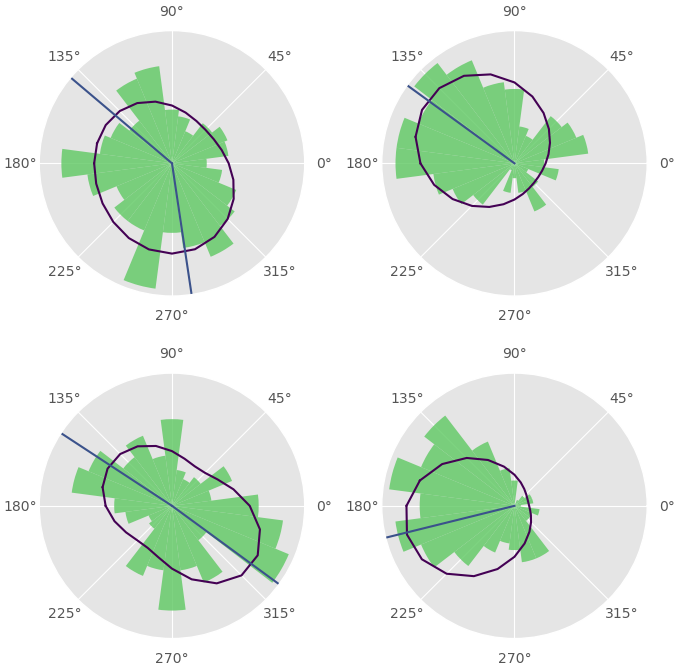

Path orientations in the experimental group

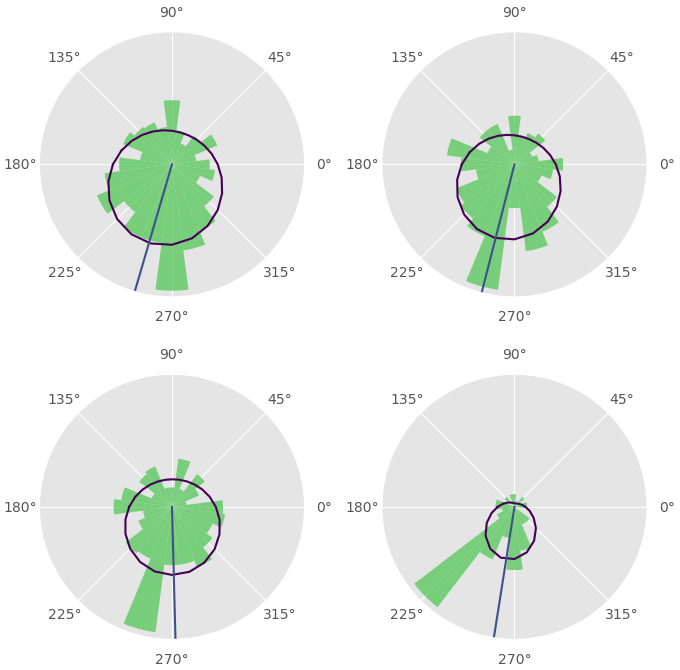

Path orientations in the control group

Figure 9: **Escape path orientations show that flies do not take the most optimal paths towards the shelter**

Heading and orientation (θ_h & θ_o respectively) relative to the shelter (°) in the first 10 frames after beginning response to stimulus

Figure 10: **Flies do not preferentially turn towards the shadow during initiation of escape**

Flies appear to escape mainly away from the stimulus but biasing their escape trajectory towards the shadow. We proceeded to analyse the trajectories of flies that reached the shelter after escape. A small number of flies actually reached the shadow after removing trajectories where the fly circled the entire arena before reaching the shadow (11) hence a statistical analysis is not possible due to small sample size. However visually these trajectories appear to be straighter (i.e. have lower tortuosity) and more optimal (i.e. the length of the path taken was closer to the shortest distance to the shadow) compared to the control for each stimulus presented.

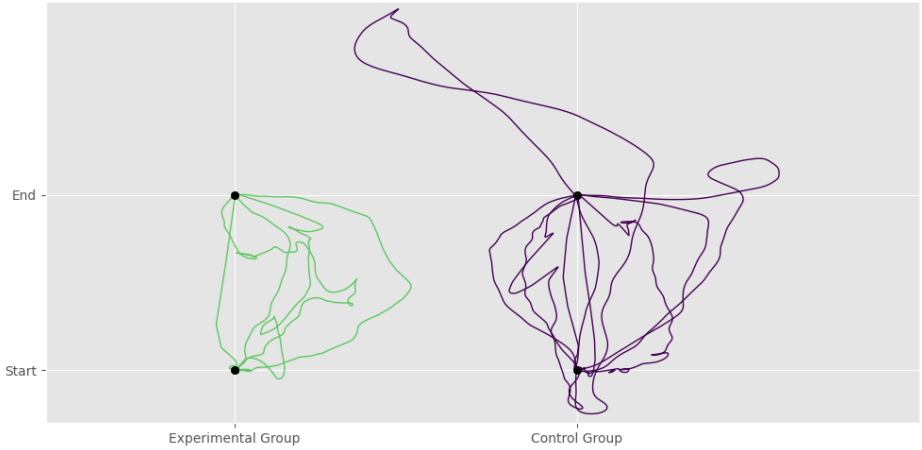

Normalized and resampled trajectories of flies reaching the shelter

Figure 11: **Flies do not take straight paths towards shelter**

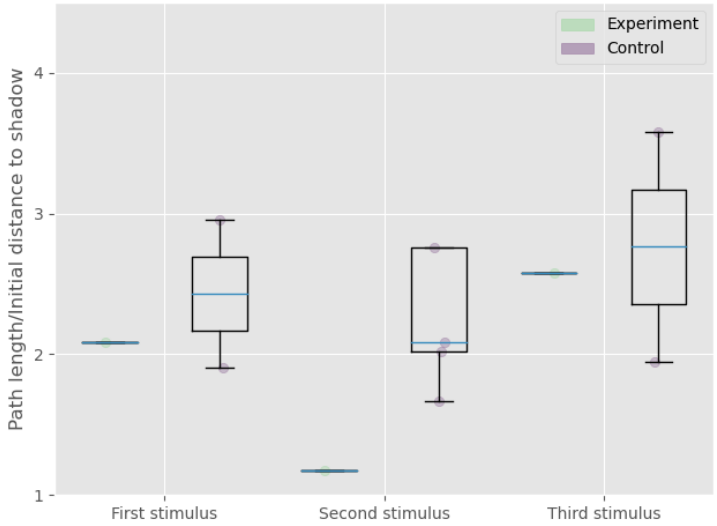

Ratio of path length and shortest distance to shelter

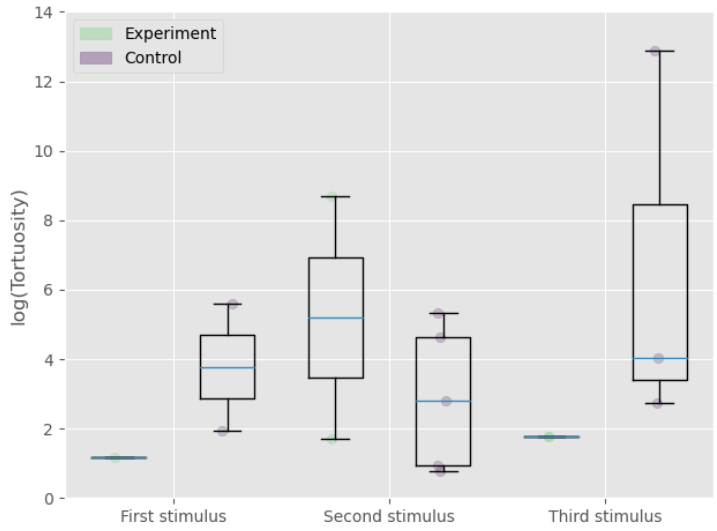

Semi-log plot of tortuosity of escape paths of flies reaching the shelter

Figure 12: **Flies appear to take more optimal paths towards the shadow compared to the control**

We also looked at the time taken for flies to reach the shelter with consecutive stimuli (13). Visually it appears that flies take less time to reach the shelter with increasing stimuli presentations. However this trend is also observed for the control group, and the low sample size precludes statistical analysis. To see the effect of the shelter in periods between stimuli presentations, we observed that flies spent significantly more time in the shadow

compared to the control (Kruskal-Wallis H test, $p < 0.001$). Since the shelter location is actually dependent on the stimulus direction, higher time spent around the post before the first stimulus suggests strong attraction for the post and the area around it which may or may not imply a perceived "safety" in that region.

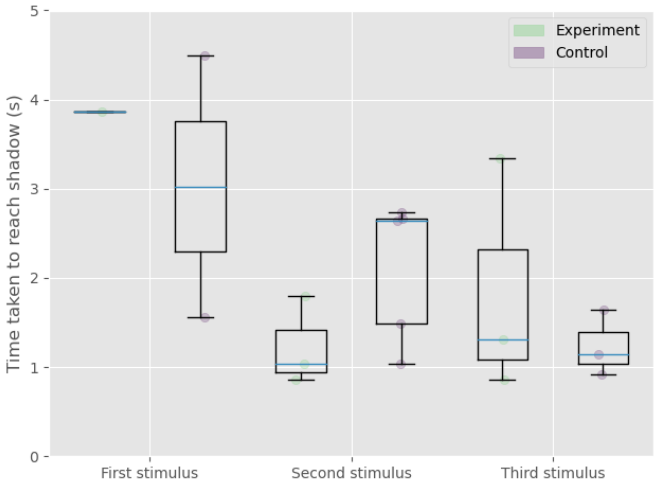

Time taken to reach the shadow

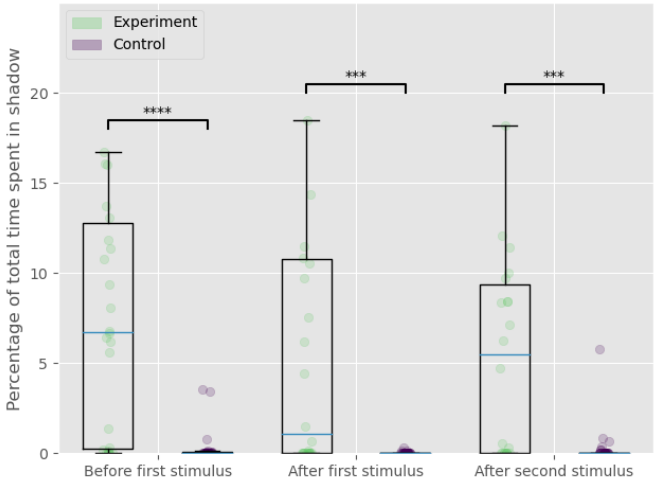

Time spent in the shadow between stimulus presentations, Kruskal-Wallis H test *** $p < 0.001$

Figure 13: **Flies reach the shelter faster with increasing number of stimuli and spend more time inside between stimulus presentations**

3.2 Behaviour in environments with potential shelter - Type B ("overhang")

The predicted "shelter" or "safe space" for this shelter design is the area directly underneath the extension. This area is dark, both due to the shadow it casts over the floor as well as the black tape covering this area. The proximity of the fly to the overhang did not influence the choice of behaviour except in one behavioural subgroup (14). Unlike the previous shelter, the distribution of speeds prior to stimulus presentation was not significantly different between the control and experimental groups (14).

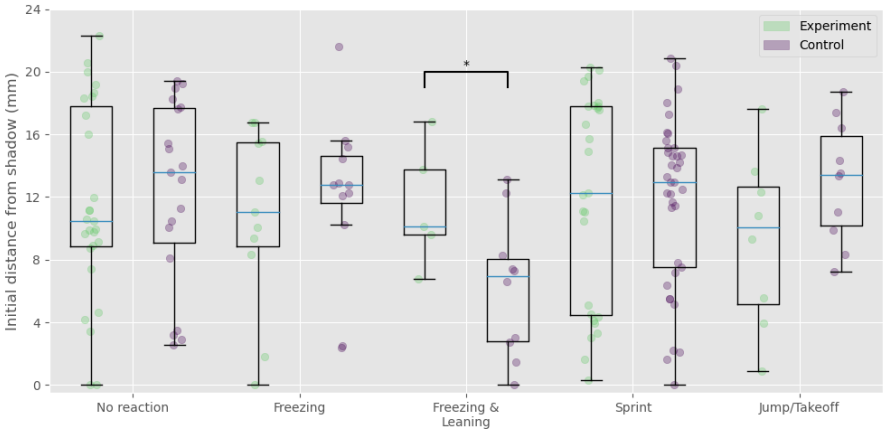

Distance from shelter immediately prior to stimulus presentation, one-way ANOVA $*p < 0.05$

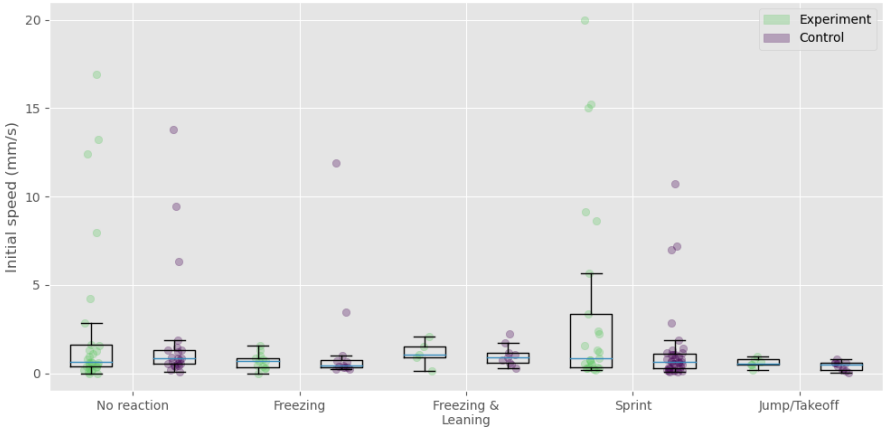

Speed immediately prior to stimulus presentation

Figure 14: **Flies don't alter their choice of behaviour in the presence of an overhang.**

The escape path orientations (θ_p) appear to be bimodal (15). Flies in the top half of the arena escape away from the stimulus as well as towards the shelter ($\mu = 260°, 360°$), while flies in the bottom half of the arena escape away from the stimulus with a slight shelter-directed bias ($\mu = 307°$). In the control group, flies mainly escape away from the stimulus with slight biases away from where the shelter would have been. With regards to microscale movements, no significant shelter-directing heading or orientation within the first 10 frames is observed (16). Like the previous shelter design, these results imply a directional bias towards the shelter, which is supported by exact trajectories that flies take albeit not without a few caveats.

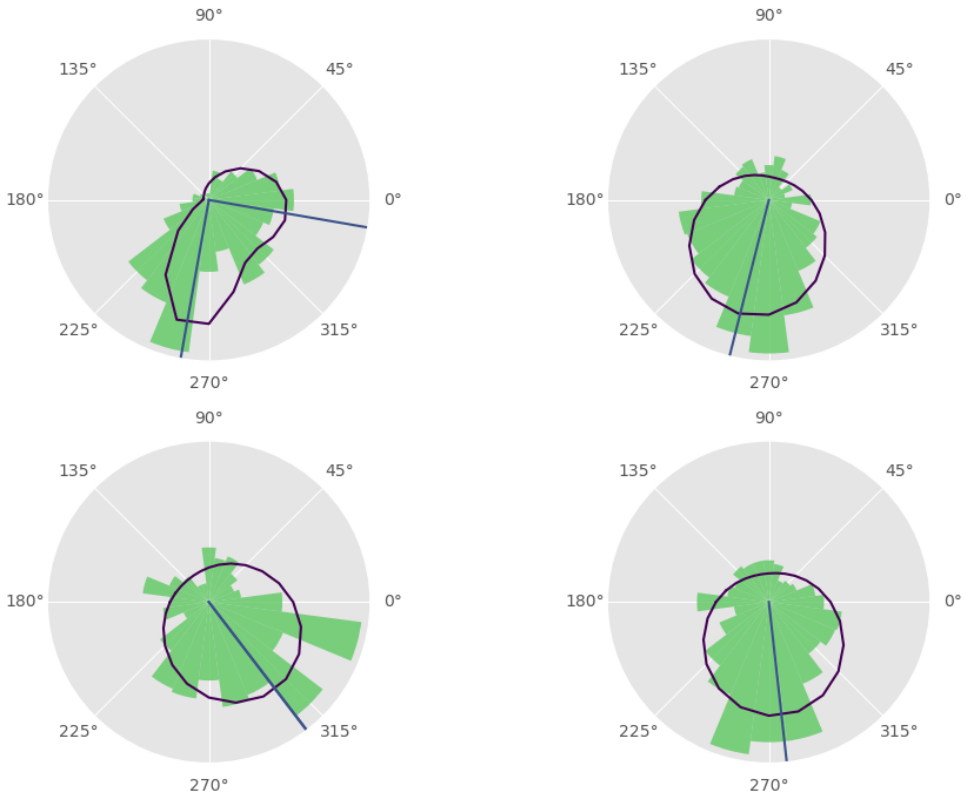

Figure 15: **Flies bias their escape direction towards shelter but still primarily escape away from stimulus.** Top and bottom correspond to top half and bottom half of the arena respectively.

Escape trajectories of flies reaching the shelter at a glance appear much straighter relative to the control, in the sense that the deviation from the

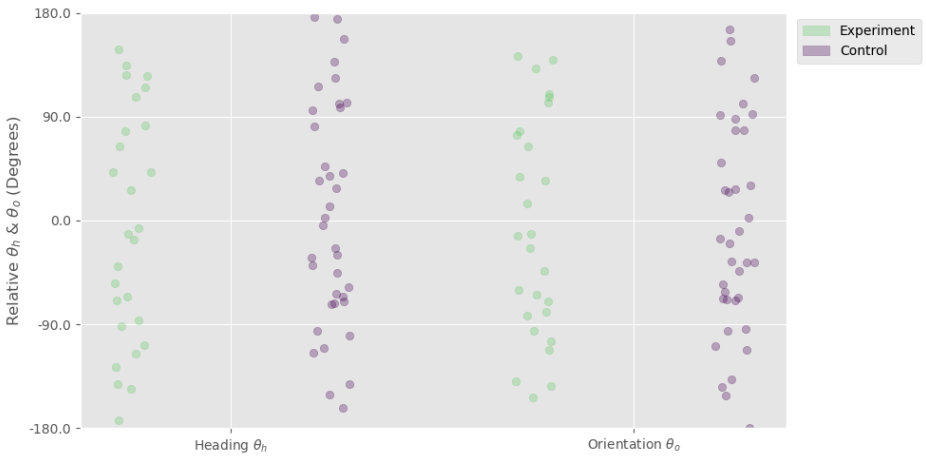

Heading and orientation (θ_h & θ_o respectively) relative to the shelter (0°) in the first 10 frames after begining response to stimulus

Figure 16: **Flies do not preferentially turn towards the shelter during initiation of escape**

ideal striaght-line trajectory towards the shelter is larger in the latter (17). However these trajectories are not "direct" or optimal in general by any measure. After each stimulus presentation the paths for flies with access to the overhang are more optimal, and (barring the first stimulus) also less tortuous compared to the control (18). However the low sample size precludes any statistical analysis for comparing medians and variances of these variables.

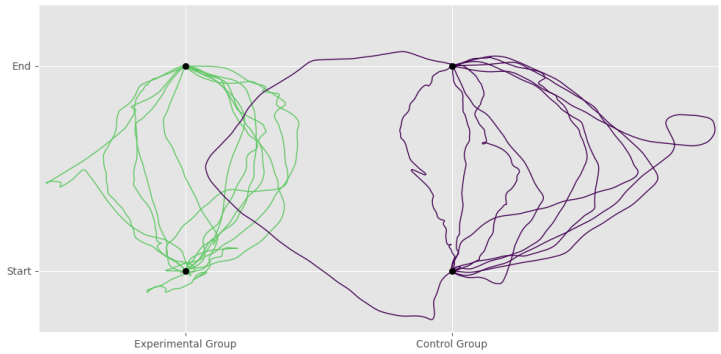

Normalized and resampled trajectories of flies reaching the shelter

Figure 17: **Flies take straighter paths towards shelter relative to the control**

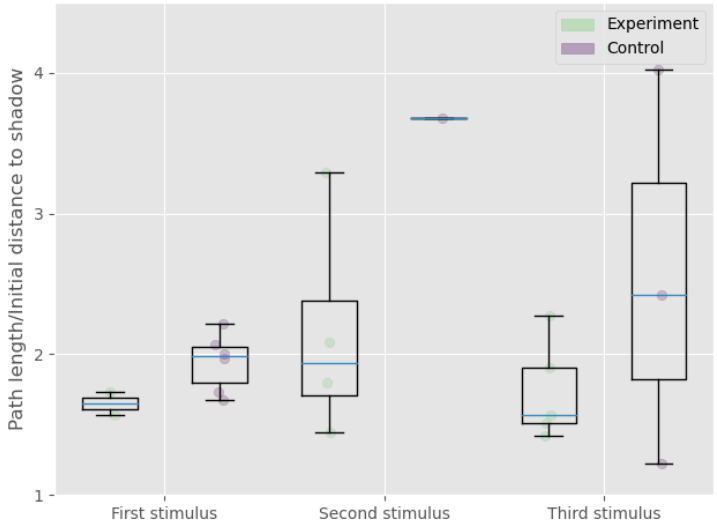

Ratio of path length and shortest distance to shelter

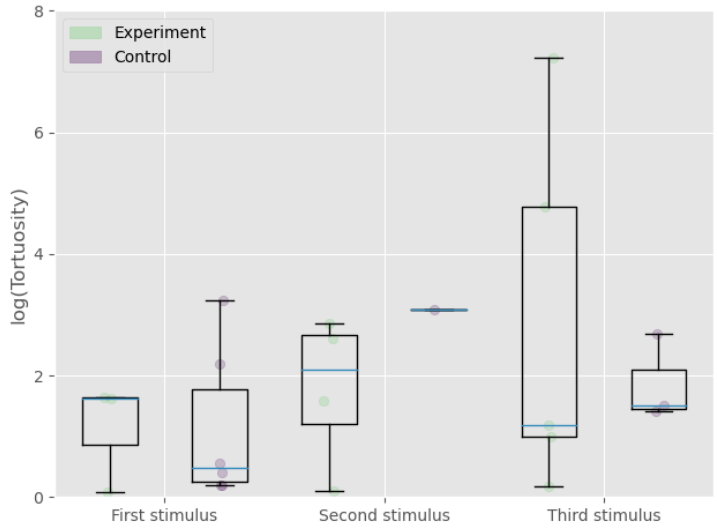

Semi-log plot of tortuosity of escape paths of flies reaching the shelter

Figure 18: **Flies do not take the most optimal paths towards the shelter, but are more optimal relative to the control**

Similarly, they appear to be generally quicker at reaching the shelter and also spend significantly more time inside the shelter relative to the control (19). The median time spent inside the shelter between stimulus presentations increases with increasing number of stimuli, which is not expected if the flies habituate to the the stimulus but instead if the flies increase their

chances of the threat disappearing by spending more time inside the shelter. Thus this is by far the most promising shelter-like arena among the ones tested.

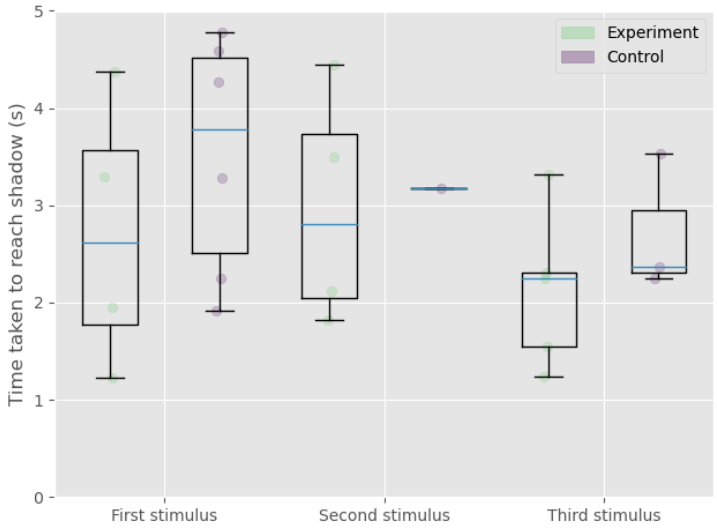

Time taken to reach overhang for the experimental group and location of the entrance of the virtual alcove for the control

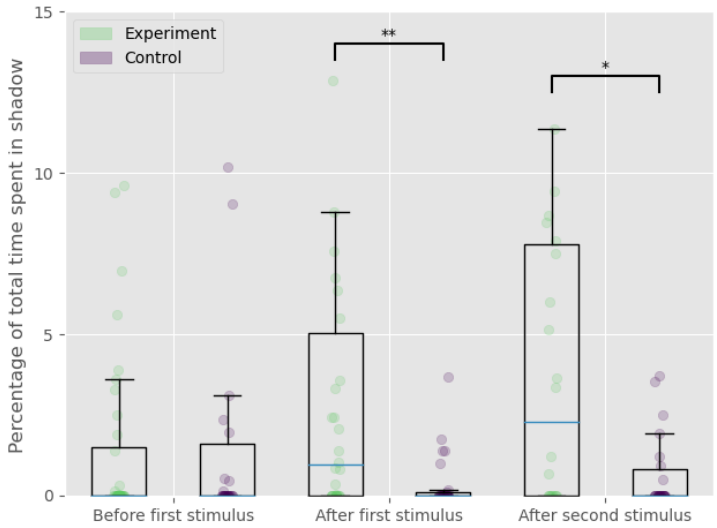

Time spent underneath the overhang between stimulus presentations, Kruskal-Wallis H test * $p < 0.05$, ** $p < 0.01$

Figure 19: **Flies reach the shelter faster but the difference in time increases with increasing number of stimuli**

3.3 Behaviour in environments with potential shelter - Type C ("alcove")

The motivation for this shelter design was the fact that flies innately prefer dark corners ((Maimon *et al.*, 2008; Soibam *et al.*, 2012b)) and have been shown to spend more time in alcoves in the presence of predators ((De La Flor *et al.*, 2017)). Like other shelter designs, no significant difference was found between behavioural choice and distance to shelter as well as speed for most behaviours (20). Only flies that fled from the stimulus were significantly closer to the alcove compared to the control group (Kruskal-Wallis H test, $p < 0.05$). There was no significant difference between distributions within the experimental group. Taken together these results do not convey meaningful information about how the alcove might be percieved by flies in an escape-behaviour context.

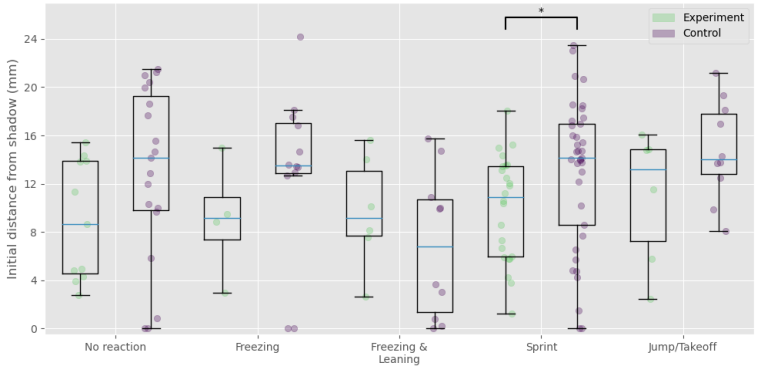

Distance from shelter immediately prior to stimulus presentation, Kruskal-Wallis H test $*p < 0.05$

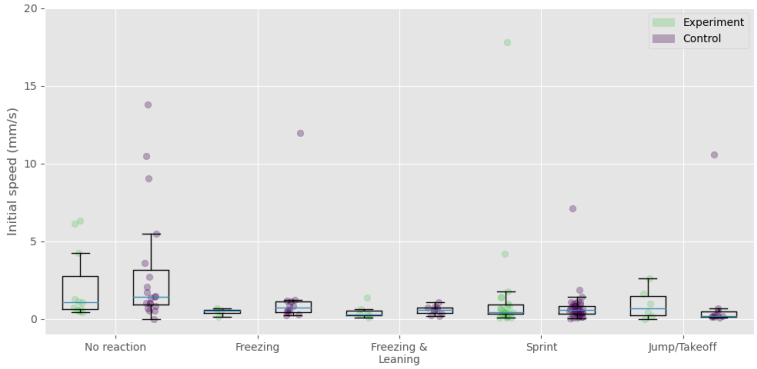

Speed immediately prior to stimulus presentation

Figure 20: **Flies don't significantly alter their choice of behaviour in the presence of alcove.**

In the presence of the alcove, escape path orientations of flies in the top half of the arena were biased towards the shelter ($\mu = 288°$), while flies in the bottom half (i.e. where escape towards shelter entails escape towards the stimulus) as well as the control group flies took paths oriented away from the stimulus (21).

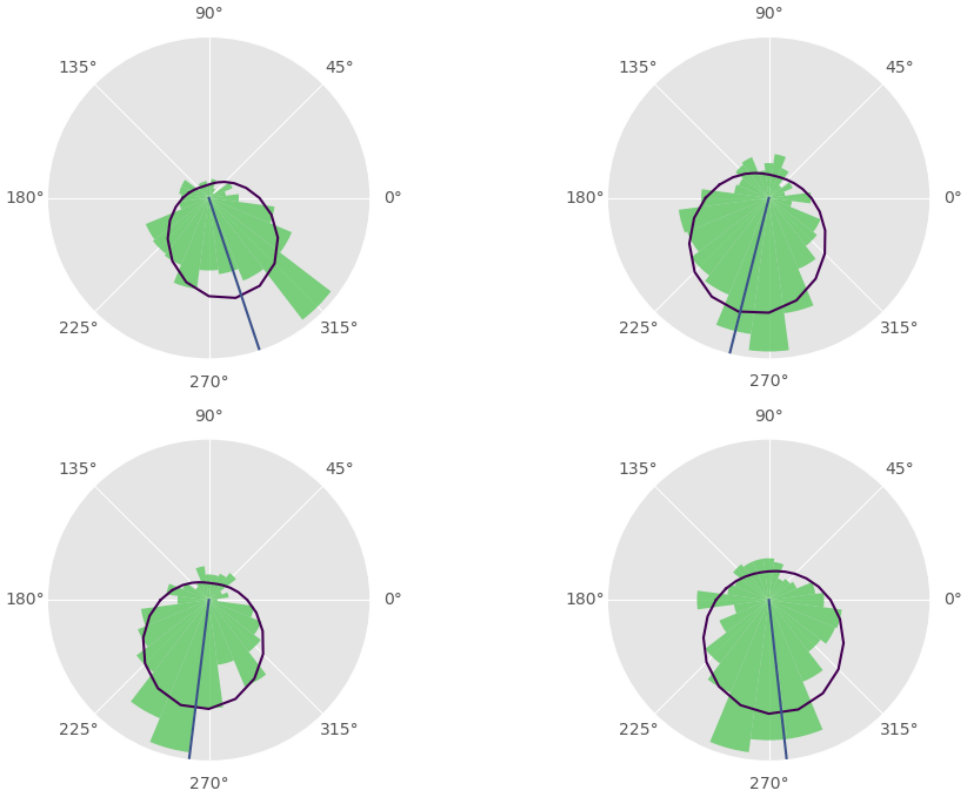

Figure 21: **Flies bias their escape direction towards shelter but still primarily escape away from stimulus.** Top and bottom correspond to top half and bottom half of the arena respectively.

This bias again does not appear to be very strong since it was not corroborated by the relative heading and orientation angles during the start of the escape (22). In the presence of the shelter, a strong shelter-directed behaviour is predicted to have relative heading and orientation angles near 0° during the initiation of the escape, since the animal is predicted to "turn" towards the shelter before escaping towards it. The almost-uniform distribution of both angles (Rayleigh's test, $p = 0.147, 0.256$ for θ_h & θ_o respectively) mean that flies do not preferentially turn towards the shelter at the start of their escape.

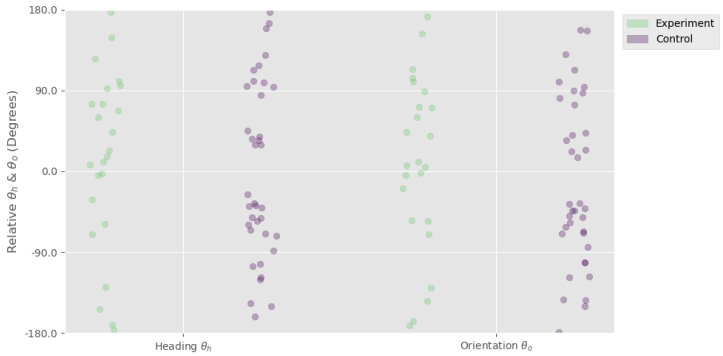

Heading and orientation (θ_h & θ_o respectively) relative to the shelter (°) in the first 10 frames after begining response to stimulus

Figure 22: **Flies do not preferentially turn towards the shelter during initiation of escape**

The escape trajectories of flies reaching the alcove (23) are not straight paths but appear to be very curved and meandering, not dissimilar to trajectories from the control group. The escape trajectories are also not particularly straight or optimal for a shelter-directed phenotype (23, 24). The low sample size for flies that ended up in the shelter prevents a detailed statisical comparison of medians and variances, but it appears that escapes towards the shelter are more tortuous and more-or-less equally optimal (i.e. the ratio

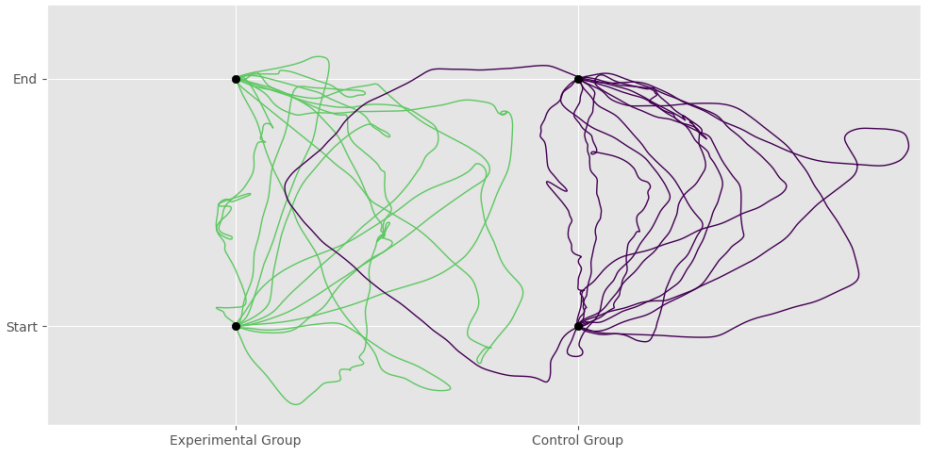

Normalized and resampled trajectories of flies reaching the shelter

Figure 23: **Flies do not take straight paths towards shelter**

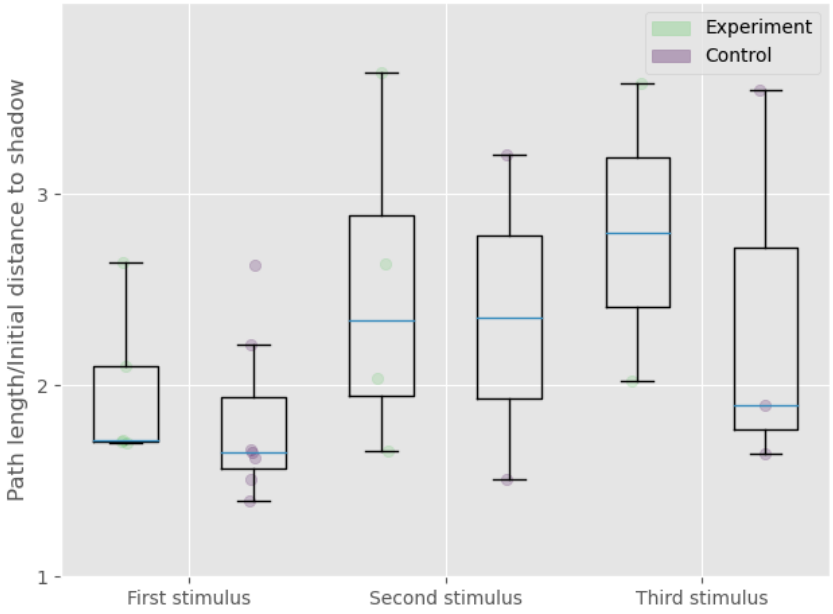

Ratio of path length and shortest distance to shelter

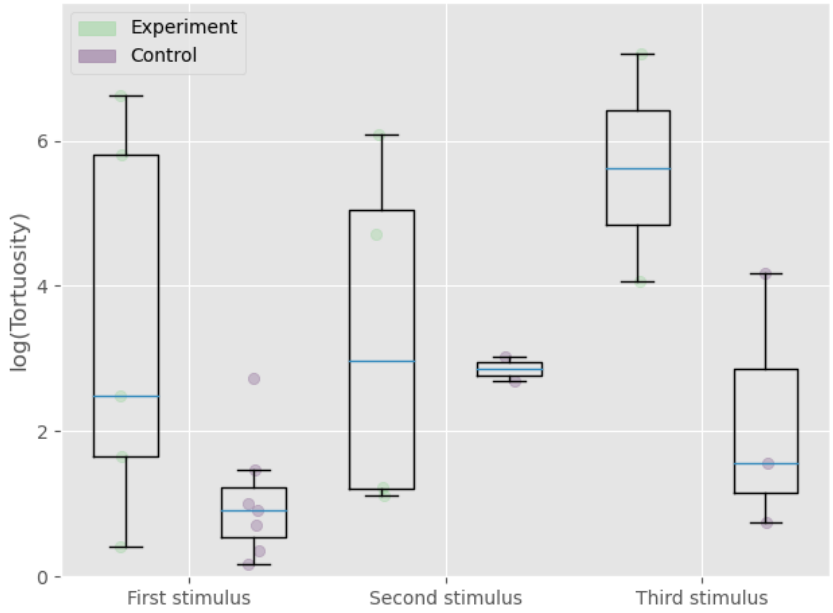

Semi-log plot of tortuosity of escape paths of flies reaching the shelter

Figure 24: **Flies do not take the most optimal paths towards the shelter**

between path length and shortest distance to the shelter is greater than 1)

compared to the control. However flies reach the shelter significantly more quickly after the first stimulus, albeit with the difference between experimental and control groups decreased with increasing number of stimuli presentations (25). This suggests that flies either got habituated to the stimulus and/or decreased the "safety" value associated with the shelter (although the results overall suggest a weak "safety" association to begin with). The low sample size prevents from a statistical comparison of the medians for higher number of stimulus presentations. Since the control arena did not actually contain a physical alcove and the virtual location of one is outside the arena, only the entrance of the alcove (which is located on the boundary of the arena and is hence also accessible to the flies in the control arena) was used as a proxy for this analysis. For the same reason it is not possible to compare the time spent in this region in the periods between stimulus presentations.

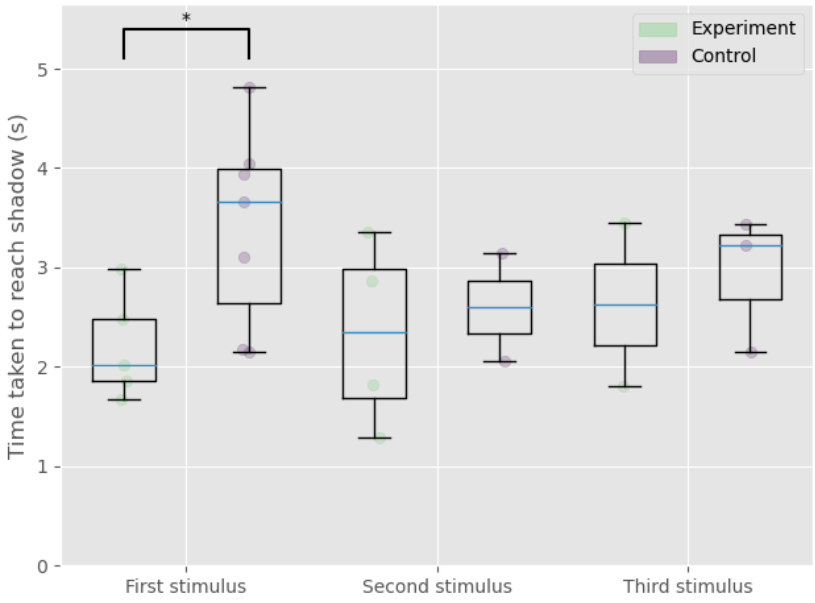

Time taken to reach alcove for the experimental group and location of the entrance of the virtual alcove for the control, $*p < 0.05$.

Figure 25: **Flies reach the shelter faster but the difference in time increases with increasing number of stimuli**

4 Conclusion

4.1 Flies flee away from the stimulus in environments without notable landmarks

Our results show that in open areas, flies flee directly away from the stimulus, which is a novel result as previous work only focused on takeoff directions as a proxy for long-term trajectories ((Card and Dickinson, 2008; von Reyn *et al.*, 2014)). This result supports the naive prediction from takeoff data and what one naturally expects regarding escape from threat. It is likely that the neural underpinnings of this behaviour is different from those corresponding to take-offs ((Dombrovski *et al.*, 2023)), since activation of DNp09 descending neurons drives both freezing and fleeing behaviour, while take-offs are mediated by the giant fibre (GF) neurons and parallel pathways ((Zacarias *et al.*, 2018; von Reyn *et al.*, 2014)).

4.2 Flies bias their escape towards shelters but do not show optimal shelter-directed trajectories

As far as the shelter designs we tested are concerned, flies bias their trajectory towards the shelter while still primarily escaping away from the stimulus. Important to note, however, is the result that multi-modal directions were still occasionally observed for certain shelter designs and relative locations of the flies in the arena. This result contradicts the observations from takeoff directions, which are distinctly bimodal - flies either jump away from the stimulus or towards the dark wedge that might be perceived as the shelter. This contradiction is expected to arise because of the difference in escape behaviours being compared. To our knowledge, there is no work comparing the two behaviours in the context of looming stimuli, and thus, we can only speculate on the similarities and dissimilarities. Takeoffs and fleeing behaviours are likely to have different neural underpinnings and thus different effects on the animal's visual processing as well as motor output ((Dombrovski *et al.*, 2023; Zacarias *et al.*, 2018; von Reyn *et al.*, 2014)).

The bias in escape directions does not imply an obvious shelter-directed behaviour akin to rodents ((Vale *et al.*, 2017)). Rather than straight trajectories ending up in the shelter, we observed a wide range of tortuosities and optimality of trajectories. This difference between species can be attributed to the high time cost of computing a trajectory towards the shelter. Walking flies internally compare heading with the goal heading on a moment-

to-moment basis ((Green *et al.*, 2019; Green and Maimon, 2018)). However, this goal-directed behaviour is processed in the central complex region of the fly brain. This region is not directly connected to visual neurons but rather receives input of visual information via 1-2 other brain regions ((Wu *et al.*, 2016; Omoto *et al.*, 2017; Namiki and Kanzaki, 2016; Otsuna and Ito, 2006). It is possible that a shelter-directed trajectory emerges over time and the primary behavioural reaction of the fly is to flee away from the stimulus while the shelter-direction is being computed in the central complex. If this were true our results might only show the initial stages of this change towards a shelter-directed strategy. This hypothesis is supported by our results showing that flies did not change their heading and orientation towards the shelter in the first 60ms after stimulus presentation. Stronger evidence for this hypothesis can be obtained by observing fly trajectories in larger environments where there is more physical space to show the changing priority over the duration of the escape, as well as observing the fly over a longer period of time. In our setup flies often quickly reached the boundary of the arena and stayed close to it, altering what in a larger arena would have been a more natural trajectory. This confound is one of the reasons why path directions were analysed only in a short period when the maximum activity took place, to counter the effects of flies simply following the edge towards the shelter.

An alternative hypothesis is that flies do not show shelter-directed behaviours at all, and the bias observed in our results is due to the landmarks associated with the shelter being visually attractive to the animal for purposes other than "safety". This hypothesis is supported by data that for shelters A and B, flies appeared to be generally attracted to the stimulus and spend more time in its vicinity compared to the control. While flies are certainly attracted to dark objects, the behavioural relevance of this attraction, not shelter or safety associated, is hard to ascertain. The shelters did not contain food-associated or mate-associated odours or signals, and between trials, the arenas were thoroughly cleaned to remove any impression or sign of previous flies. Since flies consistently spend more time inside the shelters despite this step, it is more likely that this attraction is due to a perception of safety that "dark" objects like shade or nooks represent in the flies' natural environments.

4.3 Shelter type B ("overhang") is the best candidate for observing shelter-directed behaviour in flies

Among the designs tested, escapes in the arena with shelter type B were the closest to what one might expect from shelter-directed trajectories. This shelter design had the most optimal shelter-directed trajectories, with a strong bias in path orientation towards the overhang. The low sample size precludes statistical analysis of the variables so a more conclusive statement cannot be made. However, future work should focus on this design with a larger arena size.

In conclusion, flies alter their escape when the environment contains landmarks and do not carry out a fixed reflexive reaction to the stimulus as would be naively expected from such a simple creature. However, this bias does not lead to significantly optimal trajectories towards the shelter in the short term, and shelter-directed behaviours are hypothesised to be computed and carried out over longer time frames.

5 Appendix

Behaviour	Statistical Test	Test Statistic	p value
No Reaction	Kruskal-Wallis H-test	0.082	0.774
Freezing	Kruskal-Wallis H-test	0.030	0.862
Freezing with postural adjustment	one-way ANOVA	1.316	0.271
Sprint/Fleeing	one-way ANOVA	0.005	0.939
Takeoff/Jump	one-way ANOVA	2.489	0.1082

Table 3: Mean/medians of distance to shadow immediately before stimulus presentation for environments containing the post across behavioural choices between experimental and control groups

Behaviour	Statistical Test	Test Statistic	p value
No Reaction	Kruskal-Wallis H-test	0.006	0.937
Freezing	Kruskal-Wallis H-test	7.680	0.005
Freezing with postural adjustment	Kruskal-Wallis H-test	2.722	0.098
Sprint/Fleeing	Kruskal-Wallis H-test	2.954	0.085
Takeoff/Jump	one-way ANOVA	6.216	0.5937

Table 4: Mean/medians of speed immediately before stimulus presentation for environments containing the post across behavioural choices between experimental and control groups

Group (Quadrant)	**Rayleigh's Z test p-value**	μ	κ	**Kuiper's Two-Sample Test, statistic & p-value**
Experiment (I)	$3.364\text{x}10^{-10}$	143.9°	0.683	0.3749, 0.2651
Experiment (II)	$3.017\text{x}10^{-10}$	287.1°, 150.9°	0.841, 0.617	0.625, 0.00075
Experiment (III)	$3.123\text{x}10^{-10}$	146.2°, 323.6°	1.717, 1.150	0.499, 0.024
Experiment (IV)	$3.761\text{x}10^{-10}$	193.8°	1.028	0.2916, 0.6880
Control (I)	$3.220\text{x}10^{-10}$	255.64°	0.489	0.5833, 0.0028
Control (II)	$3.137\text{x}10^{-10}$	253.6°	0.455	0.625, 0.0007
Control (III)	$3.2199\text{x}10^{-10}$	271.5°	0.452	0.6666, 0.00011
Control (IV)	$6.232\text{x}10^{-10}$	261.0°	1.361	0.4166, 0.1355

Table 5: von-Mises mixture-model fits to escape path orientations for environments containing the post

Relative Angle (Group)	Rayleigh's Z test p-value
Heading (Experiment)	0.477
Heading (Control)	0.521
Orientation (Experiment)	0.407
Orientation (Control)	0.635

Table 6: Uniformity of relative heading and orientation angles

Subgroup	Statistical Test	Test Statistic	p value
First stimulus	-	-	-
Second stimulus	one-way ANOVA	2.921	0.138
Third stimulus	one-way ANOVA	0.567	0.493

Table 7: Mean/medians for time taken to reach shadow for environments containing the post between experimental and control groups

Subgroup	Statistical Test	Test Statistic	p value
First stimulus	Kruskal-Wallis H-test	22.396	$2.218\text{x}10^{-6}$
Second stimulus	Kruskal-Wallis H-test	16.899	$3.941\text{x}10^{-5}$
Third stimulus	Kruskal-Wallis H-test	14.169	0.00016

Table 8: Mean/medians for time spent in the shadow between stimulus presentations for environments containing the post between experimental and control groups

Subgroup	Statistical Test	Test Statistic	p value
First stimulus	one-way ANOVA	0.065	0.803
Second stimulus	one-way ANOVA	1.372	0.266
Third stimulus	one-way ANOVA	0.023	0.882

Table 9: Mean/medians for ratio of path lengths and shortest distance to shadow for environments containing the post between experimental and control groups

Subgroup	Statistical Test	Test Statistic	p value
First stimulus	-	-	-
Second stimulus	-	-	-
Third stimulus	-	-	-

Table 10: Mean/medians for tortuosity of escapes in the arena containing a post between experimental and control groups

Behaviour	Statistical Test	Test Statistic	p value
No Reaction	one-way ANOVA	0.187	0.6673
Freezing	one-way ANOVA	0.328	0.5725
Freezing with postural adjustment	one-way ANOVA	4.933	0.0447
Sprint/Fleeing	Kruskal-Wallis H-test	0.077	0.7804
Takeoff/Jump	one-way ANOVA	2.894	0.1082

Table 11: Mean/medians of distance to shadow immediately before stimulus presentation for environments containing the overhang across behavioural choices between experimental and control groups

Behaviour	**Statistical Test**	**Test Statistic**	**p value**
No Reaction	Kruskal-Wallis H-test	0.592	0.4441
Freezing	Kruskal-Wallis H-test	1.833	0.1757
Freezing with postural adjustment	one-way ANOVA	0.163	0.6928
Sprint/Fleeing	Kruskal-Wallis H-test	0.139	0.7085
Takeoff/Jump	Kruskal-Wallis H-test	0.284	0.5937

Table 12: Mean/medians of speed immediately before stimulus presentation for environments containing the overhang across behavioural choices between experimental and control groups

Group (Half)	**Rayleigh's Z test p-value**	μ	κ	**Kuiper's Two-Sample Test, statistic & p-value**
Experiment (Top)	$3.860\text{x}10^{-10}$	260°, 350°	6.475, 1.329	0.541, 0.0095
Experiment (Bottom)	$3.351\text{x}10^{-10}$	307°	0.971	0.249, 0.884
Control (Top)	$3.446\text{x}10^{-10}$	255°	0.819	0.291, 0.688
Control (Bottom)	$3.332\text{x}10^{-10}$	276°	0.693°	0.291, 0.688

Table 13: von-Mises mixture-model fits to escape path orientations for environments containing the overhang

Relative Angle (Group)	Rayleigh's Z test p-value
Heading (Experiment)	0.9642
Heading (Control)	0.4948
Orientation (Experiment)	0.7307
Orientation (Control)	0.2330

Table 14: Uniformity of relative heading and orientation angles

Subgroup	Statistical Test	Test Statistic	p value
First stimulus	one-way ANOVA	0.925	0.364
Second stimulus	-	-	-
Third stimulus	one-way ANOVA	1.087	0.179

Table 15: Mean/medians for time taken to reach shadow for environments containing the overhang between experimental and control groups

Subgroup	Statistical Test	Test Statistic	p value
First stimulus	Kruskal-Wallis H-test	0.092	0.760
Second stimulus	Kruskal-Wallis H-test	9.464	0.002
Third stimulus	Kruskal-Wallis H-test	5.761	0.016

Table 16: Mean/medians for time spent in the shadow between stimulus presentations for environments containing the overhang between experimental and control groups

Subgroup	Statistical Test	Test Statistic	p value
First stimulus	-	-	-
Second stimulus	-	-	-
Third stimulus	one-way ANOVA	1.698	0.240

Table 17: Mean/medians for ratio of path lengths and shortest distance to shadow for environments containing the overhang between experimental and control groups

Subgroup	Statistical Test	Test Statistic	p value
First stimulus	Kruskal-Wallis H-test	0.066	0.796
Second stimulus	-	-	-
Third stimulus	one-way ANOVA	0.199	0.654

Table 18: Mean/medians for tortuosity of escapes in the arena containing an overhang between experimental and control groups

Behaviour	Statistical Test	Test Statistic	p value
No Reaction	one-way ANOVA	2.6922	0.1120
Freezing	one-way ANOVA	1.1492	0.3018
Freezing with postural adjustment	one-way ANOVA	0.9311	0.3509
Sprint/Fleeing	one-way ANOVA	4.3320	0.0417
Takeoff/Jump	one-way ANOVA	2.5280	0.1341

Table 19: Mean/medians of distance to shadow immediately before stimulus presentation for environments containing the alcove across behavioural choices between experimental and control groups

Behaviour	**Statistical Test**	**Test Statistic**	**p value**
No Reaction	Kruskal-Wallis H-test	0.8561	0.3548
Freezing	one-way ANOVA	0.4932	0.4939
Freezing with postural adjustment	one-way ANOVA	0.1888	0.6704
Sprint/Fleeing	Kruskal-Wallis H-test	0.0961	0.7565
Takeoff/Jump	one-way ANOVA	0.0545	0.8186

Table 20: Mean/medians of speed immediately before stimulus presentation for environments containing the alcove across behavioural choices between experimental and control groups

Group (Half)	**Rayleigh's Z test p-value**	μ	κ	**Kuiper's Two-Sample Test, statistic & p-value**
Experiment (Top)	$3.777\text{x}10^{-10}$	288°	1.049	0.291, 0.688
Experiment (Bottom)	$3.631\text{x}10^{-10}$	263°	0.932	0.249, 0.884
Control (Top)	$3.446\text{x}10^{-10}$	255°	0.819	0.291, 0.688
Control (Bottom)	$3.32\text{x}10^{-10}$	276°	0.693°	0.291, 0.688

Table 21: von-Mises mixture-model fits to escape path orientations for environments containing the alcove

Relative Angle (Group)	Rayleigh's Z test p-value
Heading (Experiment)	0.1476
Heading (Control)	0.5501
Orientation (Experiment)	0.2561
Orientation (Control)	0.3046

Table 22: Uniformity of relative heading and orientation angles

Subgroup	Statistical Test	Test Statistic	p value
First stimulus	one-way ANOVA	6.063	0.033
Second stimulus	-	-	-
Third stimulus	-	-	-

Table 23: Statistical tests comparing mean/medians for time taken to reach shadow for environments containing the alcove between experimental and control groups

Subgroup	Statistical Test	Test Statistic	p value
First stimulus	Kruskal-Wallis H-test	2.3802	0.1228
Second stimulus	-	-	-
Third stimulus	-	-	-

Table 24: Statistical tests comparing mean/medians for ratio of path lengths and shortest distance to shadow for environments containing the post in the right half of the arena between experimental and control groups

Subgroup	Statistical Test	Test Statistic	p value
First stimulus	one-way ANOVA	4.8229	0.0881
Second stimulus	-	-	-
Third stimulus	-	-	-

Table 25: Mean/medians for tortuosity of escapes in the arena containing an alcove between experimental and control groups

References

Blanchard RJ, Blanchard DC (1971). Defensive reactions in the albino rat. Learning and Motivation 2(4), 351–362.

Campagner D, Vale R, Tan YL, Iordanidou P, Pavón Arocas O, Claudi F, Stempel AV, Keshavarzi S, Petersen RS, Margrie TW, Branco T (2023). A cortico-collicular circuit for orienting to shelter during escape. Nature 613(7942), 111–119.

Card G, Dickinson MH (2008). Visually Mediated Motor Planning in the Escape Response of Drosophila. Current Biology 18(17), 1300–1307.

Card GM (2012). Escape behaviors in insects. Current Opinion in Neurobiology 22(2), 180–186.

Catania KC (2009). Tentacled snakes turn C-starts to their advantage and predict future prey behavior. Proceedings of the National Academy of Sciences of the United States of America 106(27), 11183–11187.

Catania KC (2010). Born knowing: Tentacled snakes innately predict future prey behavior. PloS One 5(6), e10953.

De La Flor M, Chen L, Manson-Bishop C, Chu TC, Zamora K, Robbins D, Gunaratne G, Roman G (2017). Drosophila increase exploration after visually detecting predators. PLOS ONE 12(7), e0180749.

Dill LM (1974). The escape response of the zebra danio (Brachydanio rerio) I. The stimulus for escape. Animal Behaviour 22(3), 711–722.

Dombrovski M, Peek MY, Park JY, Vaccari A, Sumathipala M, Morrow C, Breads P, Zhao A, Kurmangaliyev YZ, Sanfilippo P, Rehan A, Polsky J, Alghailani S, Tenshaw E, Namiki S, Zipursky SL, Card GM (2023). Synaptic gradients transform object location to action. Nature 1–9.

Eaton RC, Lee RKK, Foreman MB (2001). The Mauthner cell and other identified neurons of the brainstem escape network of fish. Progress in Neurobiology 63(4), 467–485.

Eilam D (2005). Die hard: A blend of freezing and fleeing as a dynamic defense—implications for the control of defensive behavior. Neuroscience & Biobehavioral Reviews 29(8), 1181–1191.

Evans CS, Macedonia JM, Marler P (1993). Effects of apparent size and speed on the response of chickens, Gallus gallus, to computer-generated simulations of aerial predators. Animal Behaviour 46(1), 1–11.

Fotowat H, Gabbiani F (2011). Collision Detection as a Model for Sensory-Motor Integration. Annual Review of Neuroscience 34(1), 1–19.

Gabbiani F, Krapp HG, Laurent G (1999). Computation of Object Approach by a Wide-Field, Motion-Sensitive Neuron. Journal of Neuroscience 19(3), 1122–1141.

Gibson WT, Gonzalez CR, Fernandez C, Ramasamy L, Tabachnik T, Du RR, Felsen PD, Maire MR, Perona P, Anderson DJ (2015). Behavioral Responses to a Repetitive Visual Threat Stimulus Express a Persistent State of Defensive Arousal in *Drosophila*. Current Biology 25(11), 1401–1415.

Green J, Maimon G (2018). Building a heading signal from anatomically defined neuron types in the drosophila central complex. Current opinion in neurobiology 52, 156–164.

Green J, Vijayan V, Mussells Pires P, Adachi A, Maimon G (2019). A neural heading estimate is compared with an internal goal to guide oriented navigation. Nature neuroscience 22(9), 1460–1468.

Hassenstein B, Hustert R (1999). Hiding responses of locusts to approaching objects. Journal of Experimental Biology 202(12), 1701–1710.

Heitler WJ, Burrows M (1977). The locust jump. II. Neural circuits of the motor programme. The Journal of Experimental Biology 66(1), 221–241.

Kane GA, Lopes G, Saunders JL, Mathis A, Mathis MW (2020). Real-time, low-latency closed-loop feedback using markerless posture tracking. eLife 9, e61909.

Konschelle F (2021). Mixture of von mises disttributions.

Maimon G, Straw AD, Dickinson MH (2008). A Simple Vision-Based Algorithm for Decision Making in Flying Drosophila. Current Biology 18(6), 464–470.

Mathis A, Mamidanna P, Cury KM, Abe T, Murthy VN, Mathis MW, Bethge M (2018). DeepLabCut: Markerless pose estimation of user-defined body parts with deep learning. Nature Neuroscience 21(9), 1281–1289.

McNaughton N, Corr PJ (2004). A two-dimensional neuropsychology of defense: Fear/anxiety and defensive distance. Neuroscience & Biobehavioral Reviews 28(3), 285–305.

Namiki S, Kanzaki R (2016). Comparative neuroanatomy of the lateral accessory lobe in the insect brain. Frontiers in Physiology 7, 191794.

Omoto JJ, Keleş MF, Nguyen BCM, Bolanos C, Lovick JK, Frye MA, Hartenstein V (2017). Visual input to the drosophila central complex by developmentally and functionally distinct neuronal populations. Current Biology 27(8), 1098–1110.

Otsuna H, Ito K (2006). Systematic analysis of the visual projection neurons of drosophila melanogaster. i. lobula-specific pathways. Journal of Comparative Neurology 497(6), 928–958.

Pedregosa F, Varoquaux G, Gramfort A, Michel V, Thirion B, Grisel O, Blondel M, Prettenhofer P, Weiss R, Dubourg V, Vanderplas J, Passos A, Cournapeau D, Brucher M, Perrot M, Duchesnay E (2011). Scikit-learn: Machine learning in Python. Journal of Machine Learning Research 12, 2825–2830.

Rodgers WL, Melzack R, Segal JR (1963). "Tail flip response" in goldfish. Journal of Comparative and Physiological Psychology 56(5), 917–923.

Soibam B, Goldfeder RL, Manson-Bishop C, Gamblin R, Pletcher SD, Shah S, Gunaratne GH, Roman GW (2012a). Modeling Drosophila Positional Preferences in Open Field Arenas with Directional Persistence and Wall Attraction. PLOS ONE 7(10), e46570.

Soibam B, Mann M, Liu L, Tran J, Lobaina M, Kang YY, Gunaratne GH, Pletcher S, Roman G (2012b). Open-field arena boundary is a primary object of exploration for Drosophila. Brain and Behavior 2(2), 97–108.

Speedie N, Gerlai R (2008). Alarm substance induced behavioral responses in zebrafish (*Danio rerio*). Behavioural Brain Research 188(1), 168–177.

Tammero LF, Dickinson MH (2002). The influence of visual landscape on the free flight behavior of the fruit fly Drosophila melanogaster. Journal of Experimental Biology 205(3), 327–343.

Temizer I, Donovan JC, Baier H, Semmelhack JL (2015). A Visual Pathway for Looming-Evoked Escape in Larval Zebrafish. Current Biology 25(14), 1823–1834.

Vale R, Evans DA, Branco T (2017). Rapid Spatial Learning Controls Instinctive Defensive Behavior in Mice. Current Biology 27(9), 1342–1349.

von Reyn CR, Breads P, Peek MY, Zheng GZ, Williamson WR, Yee AL, Leonardo A, Card GM (2014). A spike-timing mechanism for action selection. Nature Neuroscience 17(7), 962–970.

Williamson WR, Peek MY, Breads P, Coop B, Card GM (2018). Tools for Rapid High-Resolution Behavioral Phenotyping of Automatically Isolated Drosophila. Cell Reports 25(6), 1636–1649.e5.

Wu M, Nern A, Williamson WR, Morimoto MM, Reiser MB, Card GM, Rubin GM (2016). Visual projection neurons in the drosophila lobula link feature detection to distinct behavioral programs. Elife 5, e21022.

Zacarias R, Namiki S, Card GM, Vasconcelos ML, Moita MA (2018). Speed dependent descending control of freezing behavior in Drosophila melanogaster. Nature Communications 9(1), 3697.